Spin-polarization response functions in high-energy $(\vec{e},e',\vec{p})$ reactions

Hiroshi Ito,[1,2] S. E. Koonin,[1] and Ryoichi Seki[1,3]
[1]*W. K. Kellogg Radiation Laboratory, California Institute of Technology, Pasadena, California 91125*
[2]*Department of Physics, The George Washington University, Washington, DC 20052*
[3]*Department of Physics and Astronomy, California State University, Northridge, Northridge, California 91330*
(Received 3 June 1997)

Spin-polarization response functions for the high-energy $(\vec{e},e'\vec{p})$ reaction are examined by computing all 18 response functions for proton kinetic energies of 0.515 and 3.170 GeV from an ^{16}O target. The Dirac eikonal formalism is applied to account for the final-state interactions. It is found to yield the response functions in good agreement with those calculated by partial-wave expansion at 0.5 GeV. We identify the response functions that are dominantly determined by the spin-orbit potential in the final-state interaction. Dependence on the Dirac- or Pauli-type current of the nucleon is investigated in the helicity-dependent response functions, and the normal-component polarization of the knocked-out proton is computed. [S0556-2813(97)02912-9]

PACS number(s): 25.30.Dh, 13.60.Hb, 24.10.Jv, 24.70.+s

I. INTRODUCTION

In a hard $(e,e'p)$ reaction, involving a few GeV/c or larger momentum transfer, the knocked-out proton experiences a strong, final-state interaction because the pN cross sections are large (30–45 mb), corresponding to a mean-free path of only about 1.5 fm. However, perturbative quantum chromodynamics suggests the possibility of color transparency [1,2], in which the knocked-out proton undergoes little final-state interaction: the knocked-out proton would have a small radius of about the inverse of the momentum transfer and would be color singlet, and thus, would interact with the other nucleons in the nucleus weakly through the color Van der Waals mechanism. This possibility has received much attention theoretically [3–7] and experimentally [8–11].

Response functions for the $(e,e'p)$ reaction are affected by the final-state interaction of the knock-out proton. Once the initial nuclear wave function is known (or assumed to be known), the response functions provide information of the final-state interaction; that is, the propagation of the knocked-out proton in the nucleus. Polarization measurements in the $(\vec{e},e'p)$ and $(\vec{e},e'\vec{p})$ can provide detailed information on the final-state interaction through the polarization response functions. Polarization measurements in the GeV region are thus of great interest, and have been proposed at the Thomas Jefferson National Accelerator Facility (TJNAF) [12,13].

The polarization response functions have been theoretically investigated most thoroughly for proton energies of several hundred MeV or less [14–16]. In the GeV region, only a few calculations have been carried out for the $(\vec{e},e'p)$ and $(\vec{e},e'\vec{p})$ response functions in the last few years [17–19].

In this paper we report a systematic examination of the full set of the eighteen spin response functions for $(\vec{e},e'\vec{p})$ in the GeV region, incorporating spin-dependent, final-state interactions. We do not address the issue of the color transparency, but do calculate the response functions for protons knocked out from different nuclear orbitals and investigate their dependence on the spin-orbit interaction and the proton form factors. We also discuss briefly the response functions for $(\vec{e},e'\vec{n})$.

We employ the Dirac formulation for the bound-state wave functions and the Dirac eikonal formalism for the knocked-out proton wave function in the final state, as was done in previous work at lower energies [14–16] and in the GeV region [17–19]. We also neglect some physically important aspects such as off-shell effects and current conservation, as in the previous works. Our objective is to establish benchmark results that can be compared to more refined calculations in the future.

The Dirac eikonal formalism is expected to agree better with the rigorous partial-wave decomposition method as the energy increases. This agreement has been demonstrated for the analyzing power and spin rotation functions of proton-nucleus elastic scattering at 0.5 GeV [20]. However, it need not hold in inelastic processes. It has been noted [20] that the incoming and outgoing projectile suffers different eikonal distortions and that the Darwin term would contribute to those processes (while it does not to the elastic amplitude.) The validity of the (non-Dirac) eikonal formalism had been questioned for the (spin-independent) $(e,e'p)$ spectral density in the GeV region [21], but its validity was later confirmed [22]. In this work, we explicitly demonstrate the validity of the formalism for the spin-response functions at 0.5 GeV, by comparing the eikonal results to those by the partial-wave decomposition method. The formalism should thus be valid in the GeV region.

To be consistent with the Dirac eikonal description of the knocked-out proton, we use the Hartree mean-field wave function of the Walecka model [23] for the bound-state proton, and so neglect nuclear correlations throughout this work. There has been a debate over the significance of correlations for high-energy $(e,e'p)$ reactions [24,25], but the effects appear to be small, once other effects such as the finite range of the proton-nucleon interactions are included [25].

In Sec. II we review briefly the formalism for the $(\vec{e},e'\vec{p})$ reaction and the Dirac eikonal method. In Sec. III, the numerical results of the 18 spin-dependent response functions are presented, together with an examination of the role of the spin-orbit potential and the dependence on the electromag-

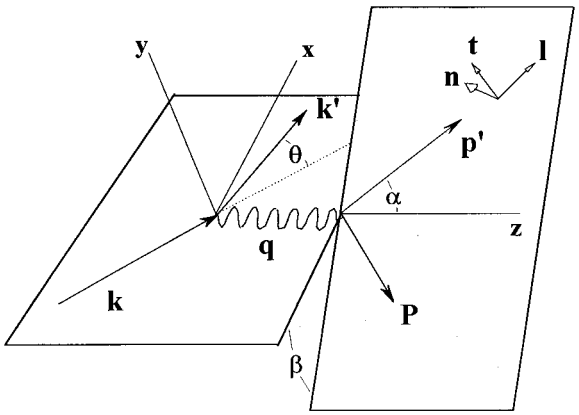

FIG. 1. The coordinate system and kinematical variables of the $(\vec{e},e'\vec{p})$ reaction. The coordinate system and the notations are the same as those used in Refs. [15] and [16].

netic current operator. A brief discussion is given in Sec. IV, and our summary and conclusions are presented in Sec. V.

II. FORMALISM FOR QUASIELASTIC ELECTRON SCATTERING

A. Spin-dependent response functions

In this work, we follow the conventions and notations for the $(\vec{e},e'\vec{p})$ kinematics that were used by Picklesimer and Van Orden [15]. For convenience, the various kinematical quantities are illustrated in Fig. 1, and are defined as follows: the four-momenta of the incoming and the outgoing electron are denoted as k and k', respectively; the photon momentum is $q=k-k'$ with $q^2\equiv q_0^2-\mathbf{q}^2<0$ (spacelike); and the four-momentum of the knocked-out proton is p'. We also take e, m_e, and M to be the electron charge, the electron mass, and the nucleon mass, respectively, and $E_{\mathbf{p}'}=(\mathbf{p}'^2+M^2)^{1/2}$ to be the on-shell energy of the proton. We follow the Bjorken-Drell convention [26] of gamma matrices and Dirac spinors, in which the normalization condition is $\overline{u(k,s)}u(k,s)=1$ for Dirac plane waves.

In the following, we sketch the formalism on which our calculation is based. It is rather standard, as described in Ref. [15], but since it is somewhat involved, we present it here for the sake of specifying notation and of clarifying the approximations involved in the quantities we calculate.

We assume (1) that the interaction between a proton in the nucleus and the electron is the one-photon exchange, and (2) that the nuclear current consists of one-body currents. We can then write the $(\vec{e},e'\vec{p})$ cross section for h and $\hat{\mathbf{s}}$, the initial electron helicity and the spin polarization of the knocked-out proton, respectively, as

$$\left(\frac{d^3\sigma}{dE_{\mathbf{k}'}d\Omega_{\mathbf{k}'}d\Omega_{\mathbf{p}'}}\right)_{h,\hat{\mathbf{s}}}=\frac{M|\mathbf{p}'|}{(2\pi)^3}\left(\frac{d\sigma}{d\Omega_{\mathbf{k}'}}\right)_{\text{Mott}}\sum_a\int dE_{\mathbf{p}'}|\mathcal{M}_a|^2\times\delta(E_{\mathbf{p}'}-q^0-M+\varepsilon_a),\tag{1}$$

summing over the occupied nuclear shell-orbits (a's) in the single-particle description of the nucleus. (ε_a is the binding energy in the a shell.) Here, the Mott cross section is

$$\left(\frac{d\sigma}{d\Omega_{\mathbf{k}'}}\right)_{\text{Mott}}=\left(\frac{e^2\cos\frac{\theta}{2}}{8\pi|\mathbf{k}|\sin^2\frac{\theta}{2}}\right)^2,\tag{2}$$

with θ the electron scattering angle. The square of the transition amplitude for the knock-out proton in the a-shell, $|\mathcal{M}_a|^2$, is written as a product of the leptonic and nuclear tensors:

$$|\mathcal{M}_a|^2=\eta_{\mu\nu}W_a^{\mu\nu}.\tag{3}$$

The leptonic tensor is defined by

$$\eta_{\mu\nu}=m^2\sum_{s_e'}[\overline{u(k,s_e)}\gamma_\mu u(k',s_e')][\overline{u(k',s_e')}\gamma_\nu u(k,s_e)]$$

$$=\frac{1}{2}(k_\mu k'_\nu+k_\nu k'_\mu-g_{\mu\nu}k\cdot k'-ih\epsilon^{\mu\nu\lambda\rho}k'_\lambda k_\rho),\tag{4}$$

where s_e and s_e' are the initial and final spins of the electron, respectively, and $\epsilon^{\mu\nu\lambda\rho}$ is the antisymmetric rank-4 tensor. Note that the electron mass is neglected in the second step of Eq. (4).

The nuclear tensor $W_a^{\mu\nu}\equiv W_a^{\mu\nu}(q;\mathbf{p}',\hat{\mathbf{s}})$ depends on q, $\mathbf{p}'$, and $\hat{\mathbf{s}}$, as well as on the quantum numbers of the a-shell orbit, and is written in terms of the matrix element of the nuclear current operator J^μ,

$$W_a^{\mu\nu}(q;\mathbf{p}',\hat{\mathbf{s}})=\sum_{j_z}J^{\mu\dagger}_{a',\hat{\mathbf{s}}}(q,\mathbf{p}')J^\nu_{a',\hat{\mathbf{s}}}(q,\mathbf{p}'),\tag{5}$$

where a' is the quantum number of the proton (that is to be knocked out) in the a-shell, including j_z, the z component of its total angular momentum. The matrix element of J_μ is given by

$$J^\nu_{a',\hat{\mathbf{s}}}(q,\mathbf{p}')=\langle\psi^{(-)}_{\mathbf{p}',\hat{\mathbf{s}}}\Psi_F(A-1,a')|j^\nu(q)|\Psi_I(A)\rangle.\tag{6}$$

Here, $\psi^{(-)}_{\mathbf{p}',\hat{\mathbf{s}}}$ is the scattered wave function of the knocked-out proton that satisfies the incoming boundary condition, $\Psi_I(A)$ is the initial, ground-state nuclear wave function, and $\Psi_F(A-1,a')$ is the final-state nuclear wave function with one hole that carries the quantum number a'; $j^\nu(q)$ is the one-body current operator, to be specified shortly.

We introduce a Möller-type operator, $\Omega^{(-)}$, that converts the Dirac plane wave to the distorted wave with the incoming boundary condition,

$$\psi^{(-)}_{\mathbf{p}',\hat{\mathbf{s}}}=\Omega^{(-)}u^{(-)}_{\mathbf{p}',\hat{\mathbf{s}}}.\tag{7}$$

Note that $\Omega^{(-)}$ is not unitary, as seen explicitly in Sec. II B.

Equation (7) now allows us to write the nuclear tensor as the diagonal element of the Dirac plane-wave spinor basis, $|u^{(-)}_{\mathbf{p}',\hat{\mathbf{s}}}\rangle$:

$$W_a^{\mu\nu}(q;\mathbf{p}',\hat{\mathbf{s}})=\text{Tr}[P_{\hat{\mathbf{s}}}(\mathbf{p}')\cdot\omega_a^{\mu\nu}(q)].\tag{8}$$

Here, the spin-projection operator $P_{\hat{\mathbf{s}}}(\mathbf{p}')$ is defined in terms of the Dirac plane-wave spinors as

$$P_{\hat{\mathbf{s}}}(\mathbf{p}')=|u^{(-)}_{\mathbf{p}',\hat{\mathbf{s}}}\rangle\langle\overline{u^{(-)}_{\mathbf{p}',\hat{\mathbf{s}}}}| \tag{9}$$

$$=\left(\frac{\not{p}'+M}{4M}\right)(1+\gamma^5\not{s}), \tag{10}$$

where the spacelike, spin four-vector s^μ is orthogonal to the momentum four-vector of the knocked-out proton and is normalized to unity. s^μ is related to the spin vector in the rest frame of the proton, $\hat{\mathbf{s}}$, as

$$s^\mu=\left(\frac{\hat{\mathbf{s}}\cdot\mathbf{p}'}{M},\ \hat{\mathbf{s}}+\frac{\hat{\mathbf{s}}\cdot\mathbf{p}'}{M(E_{\mathbf{p}'}+M)}\,\mathbf{p}'\right). \tag{11}$$

$\omega_a^{\mu\nu}(q)$ is the nuclear tensor in the Dirac plane-wave spinor space,

$$\omega_a^{\mu\nu}(q)=\sum_{j_z}\ \Omega^{(-)\dagger}\langle\Psi_F(A-1,a')|j^\nu(q)|\Psi_I(A)\rangle \times\langle\Psi_I(A)|j^{\mu\dagger}(q)|\Psi_F(A-1,a')\rangle\Omega^{(-)} \tag{12}$$

$$=s(a)\Omega^{(-)\dagger}j^\nu(q)\sum_{j_z}\ |\psi_{a'}\rangle\langle\psi_{a'}|j^{\mu\dagger}(q)\Omega^{(-)}. \tag{13}$$

Here, $\psi_{a'}$ is the single-particle wave function of the proton in the ath shell, $s(a)$ is its spectroscopic factor, and $\Omega^{(-)\dagger}$ is the adjoint of $\Omega^{(-)}$.

As we define $\hat{\mathbf{s}}$ in the rest frame of the proton, we decompose the trace in Eq. (8) in terms of the spin-polarization response functions using the (right-handed) coordinate system in that frame. We write the basis vectors of the coordinate system as $(\hat{\mathbf{n}},\hat{\mathbf{l}},\hat{\mathbf{t}})$. The spin-polarization is projected onto these vectors as $\mathcal{S}_n=\hat{\mathbf{n}}\cdot\hat{\mathbf{s}}$, $\mathcal{S}_l=\hat{\mathbf{l}}\cdot\hat{\mathbf{s}}$, and $\mathcal{S}_t=\hat{\mathbf{t}}\cdot\hat{\mathbf{s}}$. When the trace in Eq. (8) is expressed in terms of these spin projections, the spin-polarization response functions (R^n, R^l, and R^t), emerge in the coefficients of the spin projections, as seen below.

The differential cross section of the $(\vec{e},e'\vec{p})$ reaction ejecting a proton with h and $\hat{\mathbf{s}}$ is now written in its full form,

$$\left(\frac{d\sigma}{dE_{\mathbf{k}'}d\Omega_{\mathbf{k}'}d\Omega_{\mathbf{p}'}}\right)_{h,\hat{\mathbf{s}}}=\frac{1}{2}\left(\frac{d\sigma}{dE_{\mathbf{k}'}d\Omega_{\mathbf{k}'}d\Omega_{\mathbf{p}'}}\right)_h +\left[\left(\frac{d\sigma}{dE_{\mathbf{k}'}d\Omega_{\mathbf{k}'}d\Omega_{\mathbf{p}'}}\right)_{h,\hat{\mathbf{s}}} -\frac{1}{2}\left(\frac{d\sigma}{dE_{\mathbf{k}'}d\Omega_{\mathbf{k}'}d\Omega_{\mathbf{p}'}}\right)_h\right]$$

$$\equiv\frac{1}{2}\,\sigma(h,0)+\sigma(h,\hat{\mathbf{s}}), \tag{14}$$

where $\sigma(h,0)$ is the differential cross section for $(\vec{e},e'p)$ and is given by

$$\sigma(h,0)=\frac{M|\mathbf{p}'|}{(2\pi)^3}\left(\frac{d\sigma}{d\Omega_{\mathbf{k}'}}\right)_{\text{Mott}}\{v_LR_L+v_TR_T+v_{TT}R_{TT}\cos 2\beta +v_{LT}R_{LT}\cos\beta+hv_{LT'}R_{LT'}\sin\beta\}. \tag{15}$$

$\sigma(h,\hat{\mathbf{s}})$ is the polarized part of the $(\vec{e},e'\vec{p})$ differential cross section and is given by

$$\sigma(h,\hat{\mathbf{s}})=\frac{M|\mathbf{p}'|}{2(2\pi)^3}\left(\frac{d\sigma}{d\Omega_{\mathbf{k}'}}\right)_{\text{Mott}}\{[v_LR_L^n+v_TR_T^n +v_{TT}R_{TT}^n\cos 2\beta+v_{LT}R_{LT}^n\cos\beta +hv_{LT'}R_{LT'}^n\sin\beta]\mathcal{S}_n+[v_{TT}R_{TT}^l\sin 2\beta +v_{LT}R_{LT}^l\sin\beta+h(v_{LT'}R_{LT'}^l\cos\beta +v_{TT'}R_{TT'}^l)]\mathcal{S}_l+[v_{TT}R_{TT}^t\sin 2\beta+v_{LT}R_{LT}^t\sin\beta +h(v_{LT'}R_{LT'}^t\cos\beta+v_{TT'}R_{TT'}^t)]\mathcal{S}_t\}$$

$$\equiv N_n\mathcal{S}_n+N_l\mathcal{S}_l+N_t\mathcal{S}_t, \tag{16}$$

where β is the azimuthal angle of $\mathbf{p}'$ as illustrated in Fig. 1. The v's (v_L, v_T, v_{TT}, v_{LT}, $v_{LT'}$, and $v_{TT'}$) are kinematic factors, depending only on θ, $\mathbf{q}^2$, and q^2. For completeness, we list in the Appendix the relations between the response functions and the nuclear tensor, and the explicit forms of the kinematic factors.

In the experiments planned at the TJNAF, simplified kinematics is applied to reduce the number of the response functions involved: in-plane kinematics ($\beta=n\pi$) are used for polarized ($h=\pm1$)[12] and unpolarized ($h=0$)[13] beams. In the latter case, the induced polarization yields the helicity-independent (nonzero) normal polarization component. The differential cross section for this $(e,e'\vec{p})$ reaction is written in terms of the preceding $\sigma(h,0)$ and N_n (setting $\beta=n\pi$) as

$$\left(\frac{d\sigma}{dE_{\mathbf{k}'}d\Omega_{\mathbf{k}'}d\Omega_{\mathbf{p}'}}\right)=\frac{1}{2}\,\sigma(h,0)_{\beta=n\pi}[1+P_n], \tag{17}$$

where

$$P_n=[N_n/\sigma(h,0)]_{\beta=n\pi}. \tag{18}$$

In Sec. II D, we discuss our numerical results of P_n.

In this work, we use the one-body current operator in free space,

$$j^\mu(q)=\gamma^0\left[F_1(q^2)\gamma^\mu+i\,\frac{\kappa}{2M}\,F_2(q^2)\sigma^{\mu\nu}q_\nu\right], \tag{19}$$

neglecting off-shell effects involved in the current [27]. Different prescriptions for the off-shell extension of the current, as well as for recovering current conservation, have been discussed recently [28] and will be commented on in Sec. IV. In this work, we use the standard dipole form of the Dirac and the Pauli form factors, $F_1(q^2)$ and $F_2(q^2)$ (with $\kappa=1.79$), except when noted.

B. Dirac eikonal approximation

The initial- and final-state proton wave functions, $\psi_{a'}(\mathbf{r})$ and $\psi^{(-)}_{\mathbf{p}',s}(\mathbf{r})$ satisfy the Dirac equation with a scalar potential V_s, and a vector potential V_v. $\psi_{a'}(\mathbf{r})$ is the quantum-hadrodynamical wave function in the Hartree approximation [23], and is expressed in the standard form [26],

$$\psi_{a'}(\mathbf{r})=\frac{1}{r}\begin{pmatrix} iG_{n,\kappa}(r)\Phi_{\kappa,j_z}(\Omega)\\ -F_{n,\kappa}(r)\Phi_{-\kappa,j_z}(\Omega)\end{pmatrix} \tag{20}$$

for the nuclear shell state a with $a'=(n,j,l,j_z)$, where j and l are specified through a quantum number κ. The wave function is normalized to unity, and $\Phi_{\pm\kappa,j_z}$ are spin spherical harmonics with angular argument, Ω.

The continuum-state wave function of the proton with the momentum $\mathbf{p}'$ and the spin s is expressed as

$$\psi_{\mathbf{p}',s}=\begin{pmatrix} u_{\mathbf{p}',s} \\ w_{\mathbf{p}',s} \end{pmatrix}, \tag{21}$$

where each component satisfies

$$\left[\frac{-\nabla^2}{2M}+V_C+V_{\rm SO}(\sigma\cdot\mathbf{L}-i\mathbf{r}\cdot\mathbf{p}')\right]u_{\mathbf{p}',s}=\frac{\mathbf{p}'^2}{2M}\,u_{\mathbf{p}',s}$$

$$w_{\mathbf{p}',s}=-\frac{i}{D(r)}\,(\sigma\cdot\nabla)u_{\mathbf{p}',s}, \tag{22}$$

with $D(r)=E+M+V_s(r)-V_v(r)$. Here, V_C and $V_{\rm SO}$ are the central and spin-orbit potentials, related to V_s and V_v by

$$V_C(r)=V_s+\frac{E}{M}\,V_v+\frac{V_s^2-V_v^2}{2M}$$

$$V_{\rm SO}(r)=\frac{1}{2MD(r)}\,\frac{1}{r}\,\frac{d}{dr}\,[V_v-V_s]. \tag{23}$$

The solution of Eq. (22) with the incoming boundary condition is given, in the eikonal approximation, by

$$\psi^{(-)}_{\mathbf{p}',s}(\mathbf{r})=\left(\frac{E_{\mathbf{p}'}+M}{2E_{\mathbf{p}'}}\right)^{1/2}\begin{pmatrix} 1 \\ -iD(r)^{-1}(\sigma\cdot\nabla)\end{pmatrix}e^{i\mathbf{p}'\cdot\mathbf{r}}e^{iS(\mathbf{r})}\chi_s\,. \tag{24}$$

Here, $S(r)$ is the eikonal phase,

$$S(\mathbf{r})=\frac{M}{p'}\int_z^\infty dz'\{V_C(z',\mathbf{b})+V_{\rm SO}(z',\mathbf{b})[\sigma\cdot\mathbf{b}\times\mathbf{p}' -ip'z']\}, \tag{25}$$

where $\mathbf{r}=z\mathbf{e}_z+b\mathbf{e}_\perp$, with $\mathbf{e}_z$ and $\mathbf{e}_\perp$ the longitudinal and transverse unit vectors along the direction of $\mathbf{p}'$. In this work, we are interested in each contribution of the central and spin-orbit potentials to the 18 spin-dependent response functions. We implement this by switching on and off V_C and $V_{\rm SO}$ in Eqs. (24) and (25).

III. NUMERICAL RESULTS

We now describe our numerical results for the spin-dependent response functions of the $(\vec{e},e'\vec{p})$ reaction, taking ^{16}O as an example. After establishing the accuracy of the eikonal approximation (Sec. III A), we illustrate the response functions and examine effects of the final-state interaction, especially of the spin-orbit potential (Sec. III B), and effects of the nucleon electromagnetic form factors (Sec. III C). We also compute the normal-component polarization relevant to an experiment planned at TJNAF [13] (Sec. III D). Throughout Secs. III B–III D, we present results at two kinetic energies of the knock-out proton, $T_{p'}=0.515$ GeV and 3.170 GeV, corresponding to the limiting energies in the planned experiment [13]. At 0.5 GeV, we compare the response functions calculated by the eikonal and partial-wave decomposition methods.

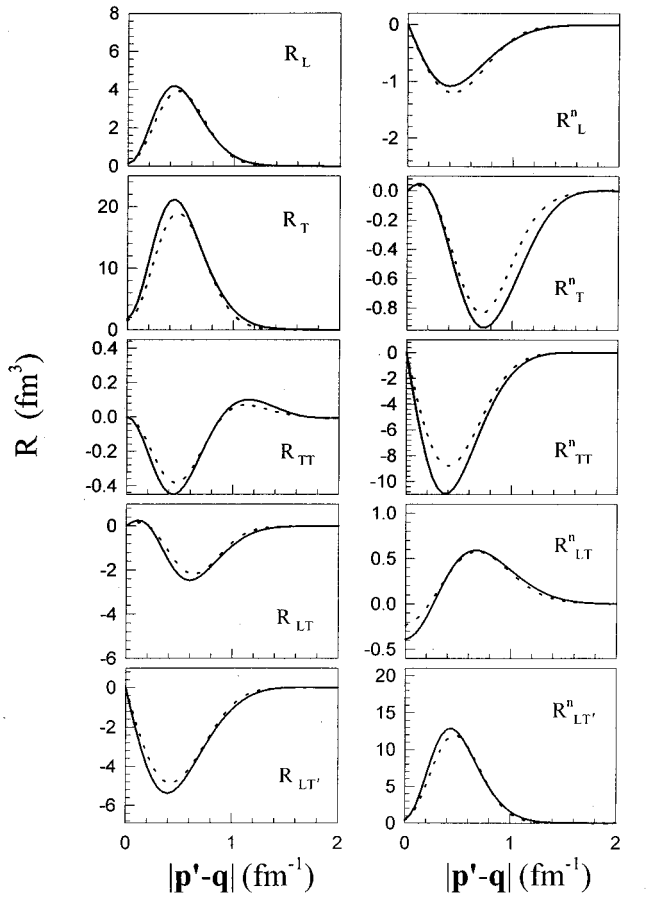

FIG. 2. Comparison of response functions calculated by the Dirac eikonal formalism (solid) and by the partial-wave decomposition method (dotted), for a proton kinetic energy of 0.5 GeV. The proton is knocked out of the $1p_{1/2}$ shell of ^{16}O. $|\mathbf{p}'-\mathbf{q}|$ is the magnitude of the recoil momentum of the residual nucleus. Both calculations use the KMT potential of Ref. [30].

A. Comparison of the eikonal approximation with partial-wave decomposition

In order to establish the accuracy of the Dirac eikonal approximation, we compare its response functions to those computed by the Dirac partial-wave decomposition method [14]. Figure 2 compares ten representative response functions (of the full 18 functions) calculated by the two methods at $T_{p'}=0.5$ GeV $(|\mathbf{p}'|=1.090\ \text{GeV}/c)$ with $Q^2\equiv -q^2=1(\text{GeV}/c)^2$. The response functions are shown in the kinematics commonly used at the low energies: as a function of the magnitude of the recoil momentum of the residual nucleus, $|\mathbf{p}'-\mathbf{q}|$, at a constant momentum transfer $|\mathbf{q}|$ with $|\mathbf{q}|=|\mathbf{p}'|$.

The response functions of the partial-wave decomposition were provided to us by Van Orden [29]. They are computed in momentum space [14] using the first-order KMT (Kerman, McManus, and Thaler) optical potential as described in Ref. [30]. In order to compare the two methods for the same input parameters and kinematics, we have converted the

momentum-space potential to coordinate-space and applied it in our eikonal calculation. Note that the Höhler nucleon electromagnetic form factor [31] was used in both calculations.

We see in Fig. 2 that the results by the two methods are quite close, within 10% at the peak for all response functions shown. The exception is R^n_{TT}, for which the discrepancy at the peak is larger (about 20%). Note that a similar, relatively large ($\sim$20%) discrepancy is seen for one of the t-component response function, R^t_{TT} (not shown here).

In order to solidify this comparison, we repeated the comparison at $T_{p'}=135$ MeV and found the discrepancy to be much larger, typically of 30–40 %, and even larger (80–100 %) for the transverse responses (R^t_{TT}, R^n_{TT}, and R^l_{TT}). (We do not exhibit the 135 MeV results in order to limit the number of figures.) As we go up to the GeV region, the number of the partial waves naturally increases, and the partial-wave decomposition method becomes more cumbersome, and eventually impractical. On the other hand, the eikonal method becomes more accurate as the ratio of $T_{p'}$ to the pN potential increases. Though we have no partial-wave decomposition results with which to compare in the GeV region, we expect that the eikonal method is reasonably accurate. Hence, the Dirac eikonal method should be a practical, reliable method for calculating final-state interactions in the high-energy $(\vec{e},e'\vec{p})$ reaction.

B. PWIA vs DWIA and effects of the spin-orbit potential

We now apply the Dirac eikonal method to examine the effects of the final-state interaction, particularly the spin-orbit potential. Here, we use the optical potential in the lowest-order impulse approximation, the so-called $f\rho$-form, where f is the free-space pN-scattering amplitude and ρ is the nuclear density taken from the Hartree mean-field nuclear wave function. Although this potential is simpler than that used in the preceding comparison of the two methods, we use it here because there is no systematic, refined potential available over the proton energy region of interest. The potentials in the Dirac eikonal method in Sec. II B are constructed [32] using pN phase-shift analyses for $T_{p'}=0.515$ [33] and 3.170 GeV [34]. A comparison of Figs. 2 and 3 shows the response functions calculated by the potential of the previous subsection and this potential are close to each other around 0.5 GeV.

Figures 3 and 4 show the complete set of 18 spin-dependent response functions for the proton knock-out from the $p_{1/2}$ shell with the kinetic energy of $T_{p'}=0.515$ GeV (the same kinematics as used in Sec. II B, $|\mathbf{p}'|=|\mathbf{q}|=1.133$ GeV/c). The response functions are calculated with and without the final-state interaction (that is, DWIA and PWIA, respectively.) The DWIA responses are generally smaller in magnitude than the PWIA responses, as a consequence of the absorption in the final-state interaction. R_T is the largest among the unpolarized response functions (R_L, R_T, R_{TT}, R_{LT}, and $R_{LT'}$), and dominates the unpolarized cross section.

The helicity-dependent response function, $R_{LT'}$, vanishes in the absence of the final-state interaction and is useful for investigating the proton-flux attenuation by the final-state interaction. At the parallel kinematics (i.e., $|\mathbf{p}'-\mathbf{q}|=0$), R_{TT}, R_{LT}, and $R_{LT'}$ vanish. At $T_{p'}=0.135$ GeV, it was observed [14] in a partial-wave decomposition calculation that the sign of R_{TT} is changed by the inclusion of the final-state interaction for the proton knocked out from the $1p_{1/2}$ shell. We find the same behavior at $T_{p'}=0.515$ and 3.170 GeV. Figure 5 shows the response functions R's and R^n's for the proton knocked out from the $1p_{3/2}$ shell. Here, R_{TT} does not change sign upon the inclusion of the final-state interaction, as is the case at $T_{p'}=0.135$ GeV [14]. The response functions for the polarized proton in the **n**, **l**, and **t** directions are also shown in Fig. 4, many of which vanish in the absence of the final-state interaction.

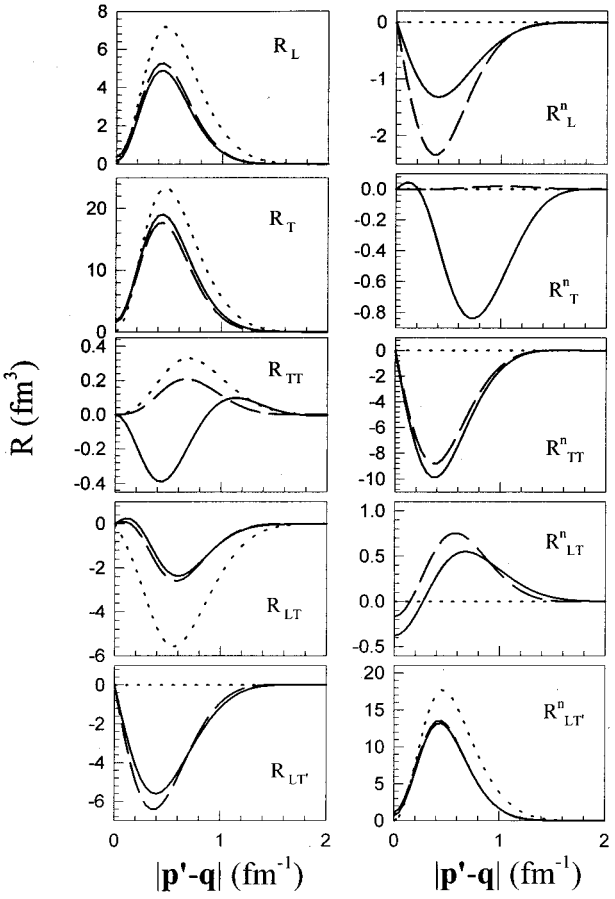

FIG. 3. Unpolarized and normal-component response functions for a proton knocked out of the $1p_{1/2}$ shell of ^{16}O with the kinetic energy of 0.515 GeV. $|\mathbf{p}'-\mathbf{q}|$ is the magnitude of the recoil momentum of the residual nucleus. Solid curves are the DWIA results by use of the Dirac eikonal formalism, and dotted curves are the PWIA results. The DWIA results with no spin-orbit potential ($V_{SO}=0$) are also shown in dashed curves. All calculations use the "$f\rho$" potential.

Figures 6 and 7 illustrate the response functions for a proton knocked out from the $1p_{1/2}$-shell at $T_{p'}=3.170$ GeV ($|\mathbf{p}'|=4.024$ GeV/c) with $|\mathbf{q}|=4.024$ GeV/c, and $Q^2=6(\mathrm{GeV}/c)^2$. They are typically smaller by two orders of magnitude relative to those at $T_{p'}=0.515$ GeV. This reduction is largely due to the Q^2 dependence of the nucleon electromagnetic form factor, the square of which is a factor in the response functions. The larger values of Q^2 expected in future experiments will reduce considerably the magnitude of

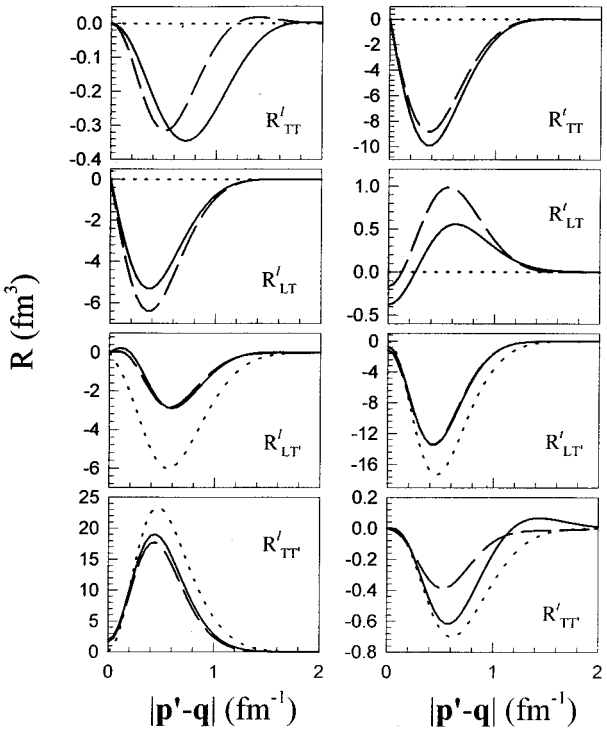

FIG. 4. Similar to Fig. 3, for the **l**- and **t**-component polarization response functions.

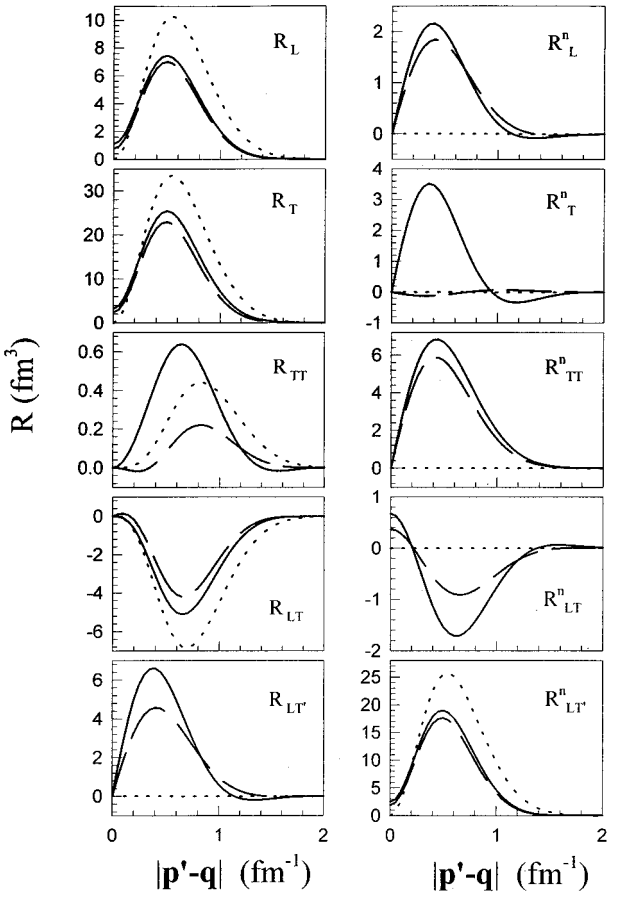

FIG. 5. Similar to Fig. 3, for a proton knocked out of the $1p_{3/2}$ shell.

the response functions to be investigated.

In order to limit the number of figures, we present here the full set of the response functions for a proton knocked out from the $1p_{1/2}$ shell at $T_{p'}=0.515$ and 3.170 GeV, which can be compared to the lower-energy results at $T_{p'}=0.135$ GeV in Ref. [16]. We also show the unpolarized and normal-component response functions (R's and R^n's, respectively) for the $1p_{3/2}$ shell, because of their greater contributions to P_n and to the spin-orbit effects than the R^l's and R^t's.

It is interesting to examine how the spin-dependent potential in the final-state interaction affects the response functions. For this purpose, we repeated the calculation omitting the spin-orbit potential from the final-state interaction ($V_{\rm SO}=0$). The resultant response functions are shown as dashed lines in Figs. 3–12. We see that the interesting sign change of R_{TT} discussed previously can be attributed to the spin-orbit potential, as is clearly demonstrated by R_{TT} in Fig. 3. The response function for the normally polarized response state, R^n_T, has a similar feature, but the plane-wave response and the response without the spin-orbit potential vanish.

In order to clarify the spin-orbit effect, we also repeated the calculation with the central potential set to zero, but leaving the spin-orbit potential intact. Figure 8 compares the three cases of the full potential, the central potential alone ($V_{\rm SO}=0$), and the spin-orbit potential alone ($V_C=0$). We see that the effect of the spin-orbit potential in the final-state interaction dominates the interference between the central and spin-orbit potential. If there were no central potential, the interesting features of R_{TT} and R^n_T described above would be enhanced. Furthermore, comparison of the response functions at the two energies in Fig. 8 shows that this effect of the spin-orbit potential (relative to the interference effect) does not decrease at the higher energy. Indeed, the effect seems to be even stronger.

Finally, we note that the sign of each response function of the $1p_{1/2}$ shell is opposite to that of the $1p_{3/2}$ shell, except for R_L, R_T, R_{LT}, and $R^n_{LT'}$.

C. Electromagnetic form factors of the nucleon

We also examine the dependence of response functions on the structure of the nucleon electromagnetic current. Figure 9 illustrates the response functions with the Dirac-type current (γ^μ) only ($F_2(q^2)=0$ and $F_1(q^2)\neq 0$), in the case of the proton knock-out from the $1p_{1/2}$ shell at $T_{p'}=0.515$ GeV. The response functions with the Pauli current ($\sigma^{\mu\nu}q_\nu$) only ($F_1(q^2)=0$ and $F_2(q^2)\neq 0$) are shown in Fig. 10. Note that the response functions shown in Fig. 3 correspond (roughly speaking) to the sum of these two (F_1 and F_2), including the interference between them. We observe that the two types of electromagnetic current are equally important for the response functions, except for the longitudinal responses R_L and R^n_L to which the Pauli current contributes little. Figures 9 and 10 also include similar calculations without the spin-orbit potential in the final-state interaction. We also observe the same feature in this case.

In the cases of the helicity-dependent response functions, $R_{LT'}$, $R^n_{LT'}$, and R_{TT}, the contributions of the Dirac-type and the Pauli-type currents have opposite signs, while the

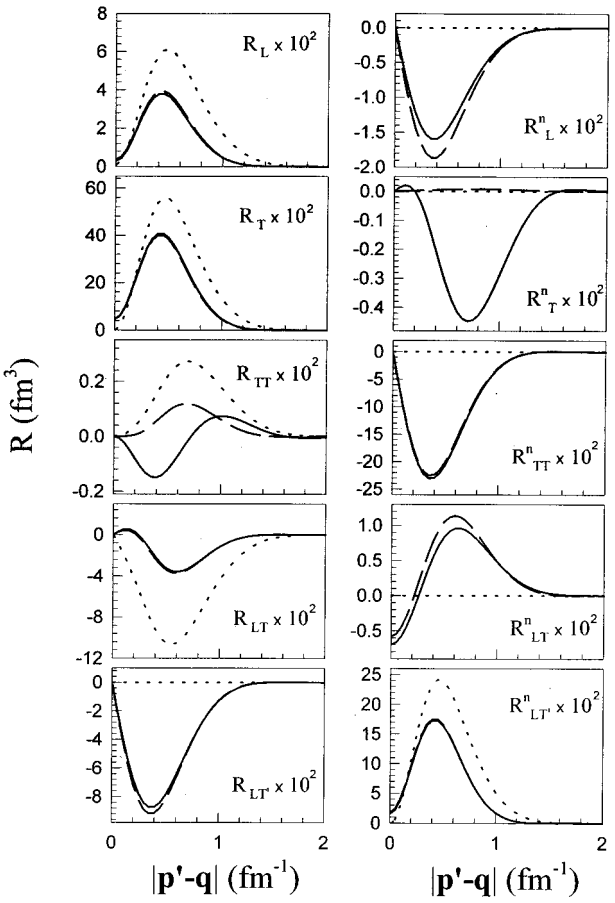

FIG. 6. Similar to Fig. 3, at a proton kinetic energy of 3.170 GeV.

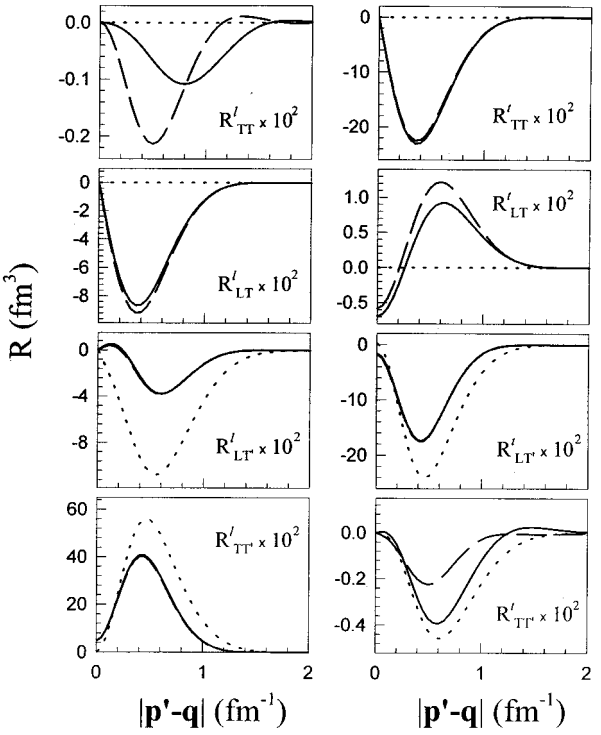

FIG. 7. Similar to Fig. 3, for the **l**- and **t**-component polarization response functions at a proton kinetic energy of 3.170 GeV.

signs remain the same in the other response functions. The neutron has a net zero charge, and its Dirac form factor is extremely small ($F_1 \simeq 0$), as is well-known from the fact that the Sachs charge radius of the neutron is almost completely saturated by the magnetic radius. The response functions shown in Fig. 10 are thus expected to be similar in sign and magnitude to the response functions for the $(\vec{e},e'\vec{n})$ reaction. We have confirmed this expectation by calculating response functions for the $(\vec{e},e'\vec{n})$ reaction with realistic neutron form factors. We are neglecting the charge-exchange contribution to the $(\vec{e},e'\vec{n})$ reaction, but this contribution is expected to be relatively small in the GeV energy region. It is interesting to note that the helicity-dependent response functions, $R_{LT'}$ and $R^n_{LT'}$, have opposite signs in $(\vec{e},e'\vec{n})$ and $(\vec{e},e'\vec{p})$.

D. Polarization of the ejected nucleon

The normal-component polarization of the outgoing proton, P_n, can be observed in the $(e,e'\vec{p})$ reaction with an unpolarized electron beam [13]. P_n is expressed in terms of of the response functions as shown in Eqs. (15)–(18). Figure 11 illustrates P_n for a proton knock-out from the the $1p_{1/2}$ and $1p_{3/2}$ shells at $T_{p'}=0.515$ GeV. In the absence of the final-state interaction, the normal spin-dependent response functions R^n_L, R^n_T, R^n_{TT}, and R^n_{LT} vanish, so that $P_n=0$ in the PWIA. P_n for the $1p_{1/2}$ shell is negative for $|\mathbf{p}'-\mathbf{q}| < 1.5$ fm^{-1}, while P_n for the $1p_{3/2}$ shell is positive for $|\mathbf{p}'-\mathbf{q}| < 1$ fm^{-1}. The polarization induced only by the central potential V_C is also shown in Fig. 11. Similar results for $T_{p'}=3.170$ GeV are shown in Fig. 12. The nuclear-recoil dependence of P_n is similar at both energies, but its magnitude is considerably smaller (by more than 40%) at $T_{p'}=3.170$ GeV than at $T_{p'}=0.515$ GeV, even becoming comparable to the expected experimental accuracy $\Delta P_n \simeq 0.5$ [13].

The polarization of the outgoing proton P_n is induced by the final-state interaction, so it vanishes in the absence of the final-state interaction. In fact, P_n is insensitive to the structure of the electromagnetic current: numerically we find P_n for the two cases, $F_1(q^2)\neq 0$ with $F_2(q^2)=0$ and $F_2(q^2)\neq 0$ with $F_1(q^2)=0$, to be practically identical.

We have also examined P_n for the $(\vec{e},e'\vec{n})$ and $(\vec{e},e'\vec{p})$ reactions at different $T_{p'}$ from different orbitals. The P_n for the two reactions are found to be almost identical, but, as noted previously, our calculation does not include the charge-exchange interaction.

IV. DISCUSSION

We briefly comment on the two important effects that we have neglected in this work.

Current conservation. A DWIA calculation of the $(\vec{e},e'\vec{p})$ amplitude suffers from the violation of current conservation. Basically, the violation arises in the truncation of the many-body degrees of freedom by restricting the current to a one-body form.

Current conservation implies a constraint on the nuclear matrix elements of the longitudinal and time components, $q^0 J^0_{\alpha,\hat{\mathbf{s}}}(q)=|\mathbf{q}|J^L_{\alpha,\hat{\mathbf{s}}}(q)$. A quantity such as $(R_L-\widetilde{R_L})/(R_L$

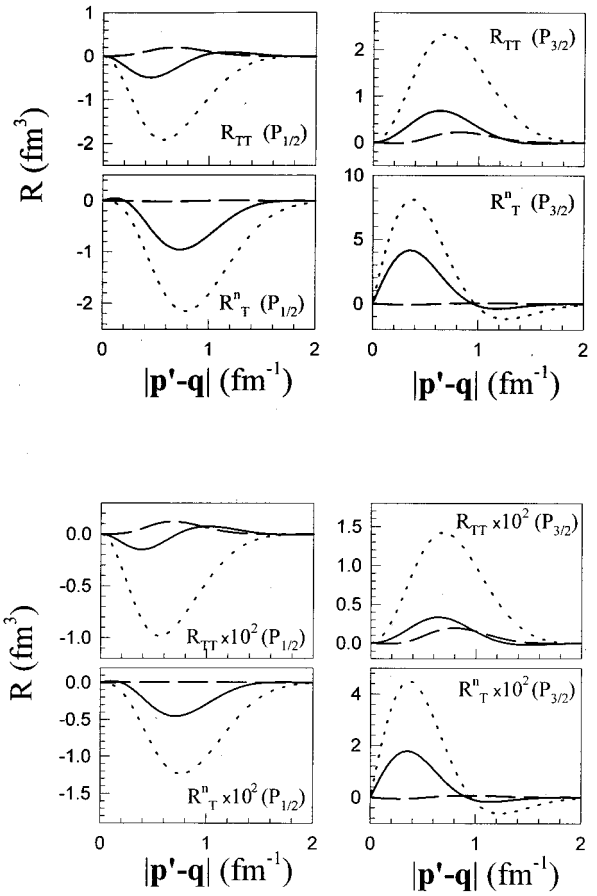

FIG. 8. Effects of spin-orbit potential in the final-state interaction. R_{TT} and R_T^n are calculated for the central potential alone ($V_{\mathrm{SO}}=0$, shown as dashed curves), for the spin-orbit interaction alone ($V_C=0$, shown as dotted curves), and for the full potential (shown by solid curves). The proton is knocked out of the $1p_{1/2}$ and $1p_{3/2}$ shells of ^{16}O with kinetic energies of 0.515 GeV (the four upper frames) and 3.170 GeV (the four lower frames). The dashed and solid curves in this figure are identical to the corresponding ones in Figs. 3, 5, and 6, but note the different scales used. As in the other figures, $|\mathbf{p}'-\mathbf{q}|$ is the magnitude of the recoil momentum of the residual nucleus.

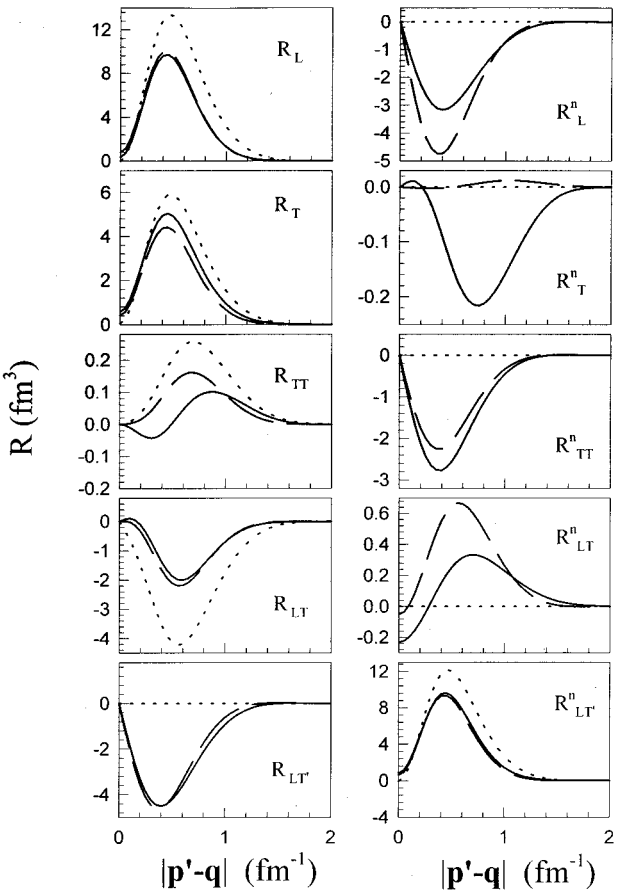

FIG. 9. Similar to Fig. 3, for the Dirac-type current $[F_1(q^2)\gamma^\mu \neq 0$ and $F_2(q^2)\sigma^{\mu\nu}q_\nu=0]$.

$+\widetilde{R_L}$) would provide a measure of the violation of this constraint [14]. Here, the longitudinal response function R_L is calculated by the use of $J^L_{\alpha,\hat{\mathbf{s}}}(q)$, and the $\widetilde{R_L}$ is by the use of $q^0 J^0_{\alpha,\hat{\mathbf{s}}}(q)/|\mathbf{q}|$. Although this measure was found to reach nearly 40% at $T_{p'}=135$ MeV [14], it has been estimated to be less than 10% for $T_{p'}>0.515$ GeV [18]. The latter high-energy estimate is comparable to other uncertainties in our calculation, such as those in the optical-potential parameters. However, the normal-component polarizations that contribute to P_n would be less affected by current nonconservation because they depend mostly on the transverse components.

Off-shell effects. The issue of the nonconserved current is complicated by off-shell effects because there is no unique way to recover current conservation for off-shell nucleons. For example, other forms of the one-body current operator $j^\mu(q)$ that are equivalent to Eq. (19) by means of the Gordon decomposition are no longer equivalent [27]. Recently, the off-shell effects for $(e,e'p)$ were estimated in PWBA to be less than 10% in the GeV region by imposing current conservation in various ways [28].

From these observations, we suspect that the physics neglected in this work could contribute appreciably. Clearly, more refined work is needed to establish reliable results.

V. SUMMARY AND CONCLUSION

In this work, we have presented a DWIA calculation of all 18 spin-polarization response functions for the $(\vec{e},e'\vec{p})$ reaction in the GeV region of proton energies. As such, we neglect some important physics such as the nuclear current conservation and the off-shell effects. The Dirac eikonal formalism used seems to agree well with the partial-wave expansion method at the relevant energies.

Our findings are summarized as follows.

(1) Effects of the final-state interaction in R_{TT} and R_T^n are dominated by the spin-orbit potential, and these response functions either vanish or almost vanish in the absence of the spin-orbit interaction. The effect in R_{TT}^n is caused mostly by the central potential. These effects occur in both the $1p_{1/2}$-shell and $1p_{3/2}$-shell knock-out processes at $T_{p'}=0.515$ GeV and 3.170 GeV.

(2) Except for the helicity-dependent $R^n_{LT'}$, each of normal-component responses of the $1p_{1/2}$ shell has the opposite sign to that of the $1p_{3/2}$ shell. P_n thus receives different contributions from the two spin-orbit partners.

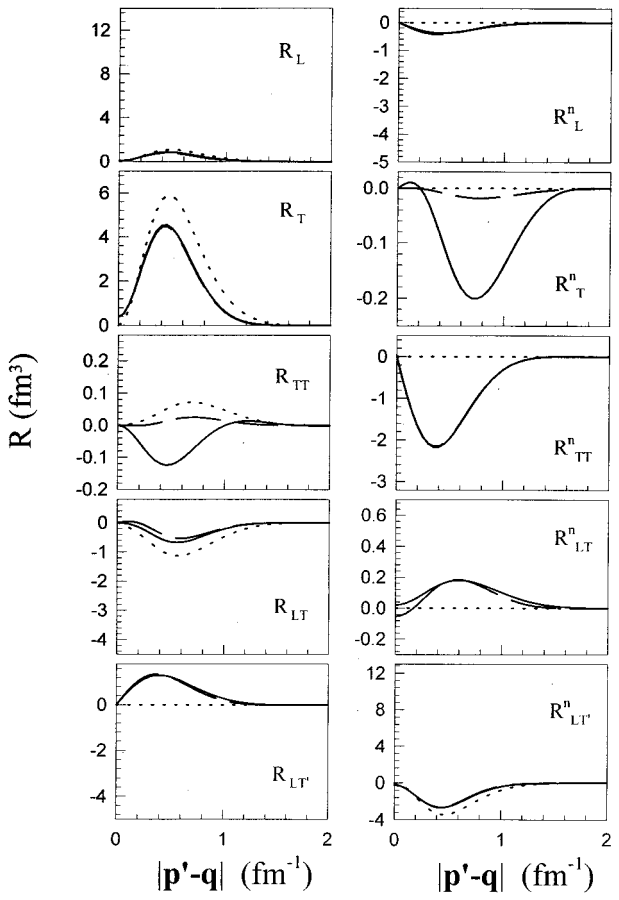

FIG. 10. Similar to Fig. 4, for the Pauli-type current $[F_1(q^2)\gamma^\mu = 0$ and $F_2(q^2)\sigma^{\mu\nu}q_\nu \neq 0]$.

(3) The response functions become smaller as Q^2 increases, mostly due to the Q^2 dependence of the electromagnetic form factor of the nucleon.

(4) Both the Dirac and Pauli currents are significant for the response functions except for the longitudinal responses R_L and R_L^n, to which the Pauli current contributes little. The two currents contribute with different signs to the helicity-dependent response functions, $R_{LT'}$ and $R_{LT'}^n$.

(5) The nonvanishing P_n attributed to final-state interactions is insensitive to the structure of the electromagnetic current operator.

We close with a speculation based on (1) above: Because R_T^n and R_{TT} vanish (or almost vanish) in the absence of the spin-orbit final-state interaction, detailed measurements of these response functions could reveal spin-dependent properties of the small, color-singlet proton that might be produced in high-energy $(e,e'p)$. So far, no serious investigation has been made of spin structure of the small proton except for a speculative description [35]. Such measurements might reveal more about this strange form of the proton, especially because most experiments are carried out at energies where the process would be incompletely controlled by perturbative QCD.

ACKNOWLEDGMENTS

We would like to acknowledge Professor J. W. Van Orden for providing response functions calculated by the partial-wave decomposition method. R. S. thanks Dr. W. R. Greenberg for clarifying symmetry properties of the response functions and G. A. Miller for useful comments which have improved the manuscript. We have benefited from a Dirac eikonal calculation of the high-energy $(\vec{e},e'p)$ reaction by Dr. A. Allder. This work was supported by the National Science Foundation grant at Caltech (PHY-9412818 and PHY-9420470), and by the U.S. Department of Energy grant at George Washington Univ. (DE-FG02-95-ER40907) and at CSUN (DE-FG03-87ER40347).

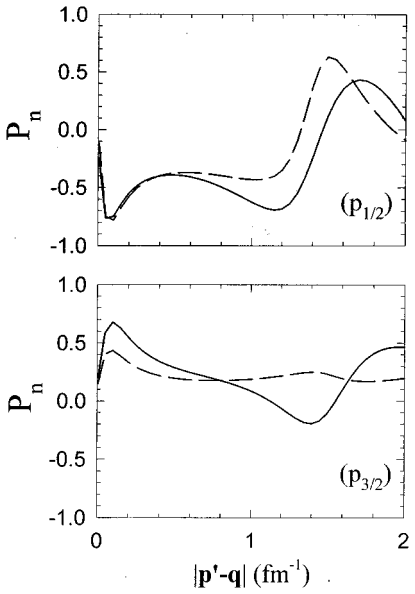

FIG. 11. The normal-component polarization, P_n, for a proton knocked out of the $1p_{1/2}$ and the $1p_{3/2}$ shells with kinetic energy $T_{p'} = 0.515$ GeV. The dashed curves are calculated with only the central potential, while the solid curves are with the full (central and spin-orbit) potential.

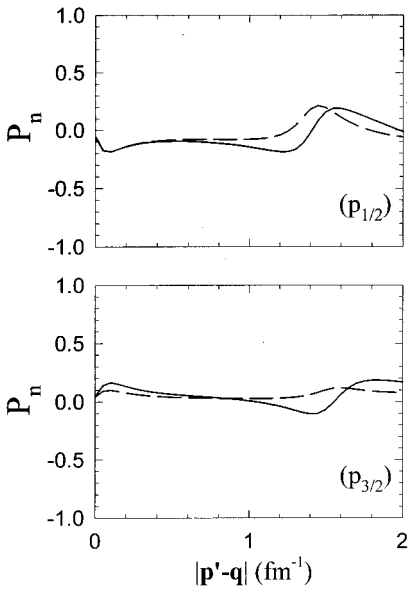

FIG. 12. Similar to Fig. 11, for a proton kinetic energy of 3.170 GeV.

APPENDIX: KINEMATIC FACTORS OF STRUCTURE FUNCTIONS

The kinematic factors, v's, in Eqs. (15) and (16) are defined to be $v_L = Q^4/\mathbf{q}^4$, $v_T = [Q^2/2\mathbf{q}^2 + \tan\theta/2]$, $v_{TT} = Q^2/2\mathbf{q}^2$, $v_{LT} = (Q^2/\mathbf{q}^2)[Q^2/\mathbf{q}^2 + \tan^2\theta/2]^{1/2}$, $v_{LT'} = (Q^2/\mathbf{q}^2)\tan\theta/2$, and $v_{TT'} = \tan\theta/2[Q^2/\mathbf{q}^2 + \tan^2\theta/2]^{1/2}$ with $Q^2 = -q^2$.

The response functions are obtained by the application of the projection operator $\mathcal{P}_{\mathbf{a}} = |\mathbf{a}\rangle\langle\mathbf{a}|\frac{1}{2}(1 + \sigma\cdot\hat{\mathbf{a}})$ for $\hat{\mathbf{a}} = \hat{\mathbf{n}}$, $\hat{\mathbf{l}}$, or $\hat{\mathbf{t}}$. More explicitly, they are given by

$$
\begin{aligned}
R_L &= \mathrm{Tr}\{\widetilde{R_L}\mathbf{I}\}, \quad & R_L^n &= \mathrm{Tr}\{\widetilde{R_L}\sigma\cdot\mathbf{n}\},\\
R_T &= \mathrm{Tr}\{\widetilde{R_T}\mathbf{I}\}, \quad & R_T^n &= \mathrm{Tr}\{\widetilde{R_T}\sigma\cdot\mathbf{n}\},\\
R_{TT} &= \mathrm{Tr}\{\widetilde{R_{TT}}\mathbf{I}\}/\cos 2\beta, \quad & R_{TT}^n &= \mathrm{Tr}\{\widetilde{R_{TT}}\sigma\cdot\mathbf{n}\}/\cos 2\beta,\\
R_{LT} &= \mathrm{Tr}\{\widetilde{R_{LT}}\mathbf{I}\}/\sin\beta, \quad & R_{LT}^n &= \mathrm{Tr}\{\widetilde{R_{LT}}\sigma\cdot\mathbf{n}\}/\sin\beta,\\
R_{LT'} &= \mathrm{Tr}\{\widetilde{R_{LT'}}\mathbf{I}\}/\cos\beta, \quad & R_{LT'}^n &= \mathrm{Tr}\{\widetilde{R_{LT'}}\sigma\cdot\mathbf{n}\}/\cos\beta,\\
R_{LT}^t &= \mathrm{Tr}\{\widetilde{R_{LT}}\sigma\cdot\mathbf{t}\}/\cos\beta, \quad & R_{LT}^l &= \mathrm{Tr}\{\widetilde{R_{LT}}\sigma\cdot\mathbf{l}\}/\cos\beta,\\
R_{TT}^t &= \mathrm{Tr}\{\widetilde{R_{TT}}\sigma\cdot\mathbf{t}\}/\sin 2\beta, \quad & R_{TT}^l &= \mathrm{Tr}\{\widetilde{R_{TT}}\sigma\cdot\mathbf{l}\}/\sin 2\beta,\\
R_{LT'}^t &= \mathrm{Tr}\{\widetilde{R_{LT'}}\sigma\cdot\mathbf{t}\}/\sin\beta, \quad & R_{LT'}^l &= \mathrm{Tr}\{\widetilde{R_{LT'}}\sigma\cdot\mathbf{l}\}/\sin\beta,\\
R_{TT'}^t &= \mathrm{Tr}\{\widetilde{R_{TT'}}\sigma\cdot\mathbf{t}\}, \quad & R_{TT'}^l &= \mathrm{Tr}\{\widetilde{R_{TT'}}\sigma\cdot\mathbf{l}\}, \qquad \text{(A1)}
\end{aligned}
$$

where the $\widetilde{R}$'s are given in terms of the nuclear tensor in the Dirac plane-wave, spinor space as

$$
\begin{aligned}
\widetilde{R_L} &= \overline{\omega}^{00},\\
\widetilde{R_T} &= \overline{\omega}^{22} + \overline{\omega}^{11},\\
\widetilde{R_{TT}} &= \overline{\omega}^{22} - \overline{\omega}^{11},\\
\widetilde{R_{LT}} &= \overline{\omega}^{20} + \overline{\omega}^{02},\\
\widetilde{R_{LT'}} &= i(\overline{\omega}^{10} - \overline{\omega}^{01}),\\
\widetilde{R_{TT'}} &= i(\overline{\omega}^{12} - \overline{\omega}^{21}). \qquad \text{(A2)}
\end{aligned}
$$

[1] A. H. Mueller, in *Proceedings of the Seventeenth Rencontre de Moriond, 1982*, edited by J. Tran Thanh Van (Editions Frontières, Gif-sur-Yvette, France, 1982), p. 13.
[2] S. J. Brodsky, in *Proceedings of the Thirteenth International Symposium on Multiparticle Dynamics*, edited by W. Kittel *et al.* (World Scientific, Singapore, 1983).
[3] G. R. Farrar, H. Liu, L. L. Frankfurt, and M. I. Strikman, Phys. Rev. Lett. **61**, 686 (1988).
[4] J. P. Ralston and B. Pire, Phys. Rev. Lett. **65**, 2343 (1990).
[5] B. K. Jennings and G. A. Miller, Phys. Rev. Lett. **69**, 3619 (1992).
[6] L. Frankfurt and M. Strickman, Prog. Part. Nucl. Phys. **27**, 135 (1991).
[7] A. Kohama, K. Yazaki, and R. Seki, Nucl. Phys. **A551**, 687 (1993).
[8] A. S. Carroll *et al.*, Phys. Rev. Lett. **61**, 1698 (1988).
[9] N. C. R. Makins *et al.*, Phys. Rev. Lett. **72**, 1986 (1994).
[10] R. McKeown and R. Milner, spokesmen, NE-18 (SLAC) collaboration.
[11] R. McKeown, Nucl. Phys. **A532**, 285c (1991).
[12] Exp. 89-033 (spokesman, C. Glashausser).
[13] Exp. 91-006 (spokesman, A. Saha).
[14] A. Picklesimer, J. W. Van Orden, and S. J. Wallace, Phys. Rev. C **32**, 1312 (1985).
[15] A. Picklesimer and J. W. Van Orden, Phys. Rev. C **35**, 266 (1987).
[16] A. Picklesimer and W. Van Orden, Phys. Rev. C **40**, 290 (1989).
[17] W. R. Greenberg, Ph.D. thesis, University of Washington, 1993.
[18] W. R. Greenberg and G. A. Miller, Phys. Rev. C **49**, 2747 (1994); **50**, 2643 (1994).
[19] A. Allder, Ph.D. thesis, California Institute of Technology, 1992.
[20] R. D. Amado, J. Piekarewicz, D. A. Sparrow, and J. A. McNeil, Phys. Rev. C **28**, 1663 (1983).
[21] A. Bianconi and M. Radici, Phys. Lett. B **363**, 24 (1995).
[22] A. Bianconi and M. Radici, Phys. Rev. C **53**, R563 (1996).
[23] B. D. Serot and J. D. Walecka, Adv. Nucl. Phys. **16**, 327 (1986).
[24] O. Benhar, A. Fabrocini, S. Fantoni, V. R. Pandharipande, and I. Sick, Phys. Rev. Lett. **69**, 881 (1992).
[25] R. Seki, T. D. Shoppa, A. Kohama, and K. Yazaki, Phys. Lett. B **383**, 133 (1996); N. N. Nikolaev, A. Szczurek, J. Speth, J. Wambach, B. G. Zakharov, and V. R. Zoller, *ibid.* **317**, 281 (1993).
[26] J. D. Bjorken and S. D. Drell, *Relativistic Quantum Mechanics* (McGraw-Hill, New York, 1964).
[27] T. D. Forest, Jr., Nucl. Phys. **A392**, 232 (1983).
[28] S. Pollock, H. W. L. Naus, and J. H. Koch, Phys. Rev. C **53**, 2304 (1996).
[29] Private communication with J. W. Van Orden.

[30] A. Picklesimer, P. C. Tandy, R. M. Thaler, and D. H. Wolfe, Phys. Rev. C **30**, 1861 (1984).
[31] G. Höhler, E. Pietarinen, I. Sabba-Stefanesen, F. Borkowski, G. G. Simon, V. H. Walther, and R. D. Wedling, Nucl. Phys. **B114**, 505 (1976).
[32] J. A. McNeil, J. R. Shepard, and S. J. Wallace, Phys. Rev. Lett. **50**, 1439 (1983).
[33] N. Hoshizaki, Prog. Theor. Phys. **60**, 1796 (1978).
[34] Y. Higuchi and N. Hoshizaki, Prog. Theor. Phys. **62**, 849 (1979).
[35] P. Jain, B. Pire, and J. P. Ralston, Phys. Rep. **271**, 67 (1996).